ACS Catalysis

Research Article

pubs.acs.org/acscatalysis

Bienzyme–Polymer–Graphene Oxide Quaternary Hybrid Biocatalysts: Efficient Substrate Channeling under Chemically and Thermally Denaturing Conditions

Omkar V. Zore,[†,‡] Ajith Pattammattel,[†] Shailaja Gnanaguru,[†] Challa V. Kumar,[*,†,‡,§] and Rajeswari M. Kasi[*,†,‡]

[†]Department of Chemistry, University of Connecticut, Storrs, Connecticut 06269-3060, United States

[‡]Institute of Materials Science, U-3136, University of Connecticut, Storrs, Connecticut 06269-3069, United States

[§]Department of Molecular and Cell Biology, University of Connecticut, Storrs, Connecticut 06269-3125, United States

Supporting Information

ABSTRACT: An example of a highly stable and functional bienzyme–polymer conjugate triad assembled on a topologically orthogonal support, layered graphene oxide (GO), is reported here. Glucose oxidase (GOx) and horseradish peroxidase (HRP) catalytic dyad were used as the model system for cascade biocatalysis. Poly(acrylic acid) (PAA) was used to covalently conjugate these enzymes, and then the conjugate has been subsequently adsorbed onto GO. The resultant nanobiocatalysts are represented as GOx-HRP-PAA/GO. Their morphology and structural characteristics were examined by transmission electron microscopy (TEM), agarose gel electrophoresis, circular dichroism (CD), and zeta potential. These robust conjugates remarkably functioned as active catalysts under biologically challenging conditions such as extreme pHs, high temperature (65 °C), and in the presence of a chemical denaturant. In one example, GOx-HRP-PAA/GO presented doubling of the K_{cat} (TON) (68×10^{-2} s^{-1}) at pH 7.0 and room temperature, when compared to the corresponding physical mixture of GOx/HRP (32×10^{-2} s^{-1}) under similar conditions. In another case, at 65 °C, GOx-HRP-PAA/GO displayed ∼120% specific activity, whereas GOx/HRP showed only 16% of its original activity. At pH 2.0 and in the presence of 4.0 mM SDS as the denaturant, GOx-HRP-PAA/GO presented greater than 100% specific activity, whereas GOx/HRP was completely deactivated under these conditions. Thus, we combined two concepts, enzyme–polymer conjugation followed by adsorption onto a 2D nanolayered material to obtain enhanced substrate channeling and excellent enzyme stability under challenging conditions. These features have never been attained by either traditional enzyme–polymer conjugates or enzyme–GO hybrids. This general, modular, and powerful approach may also be used to produce environmentally benign, biologically compatible (edible), and efficient cascade biocatalysts.

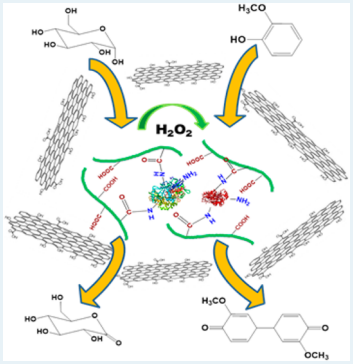

KEYWORDS: *substrate channeling, multienzyme, graphene oxide, enzyme–polymer conjugate, high temperature activity*

1. INTRODUCTION

In our quest to design and stabilize enzyme cascade dyads, we demonstrated high-temperature and pH stability of a new bienzyme catalytic quaternary hybrid assembly prepared by conjugation of two enzymes with a polymer followed by adsorption onto nanoplates of graphene oxide (GO). Glucose oxidase (GOx) and horseradish peroxidase (HRP) were used as model enzymes and poly(acrylic acid) (PAA) as the model polymer to tether the two enzymes within a network to function as an enzyme cascade dyad, Scheme 1, wherein hydrogen peroxide generated by GOx is used to oxidize a phenolic substrate by HRP.

GOx and HRP are industrial enzymes. HRP has potential uses in wastewater treatment.[1,2] GOx is used in food and baking industry and is also widely used for glucose sensing.[3] The GOx/HRP redox couple is integrated within glucose biosensors to convert chemical signal (glucose) into an electrical signal, which can be conveniently registered.[4] Furthermore, HRP coupled with other enzymes and antibodies is widely used in ELISA bioassays.[5] However, the problem is that GOx and HRP get destabilized at temperatures greater than 50 °C and have a narrow pH range (4.5–6) for retention of catalytic activity.[2,6−8] Thus, numerous methods to stabilize GOx and HRP to keep them active at biologically challenging conditions were developed. These methods include adsorption onto enzyme–polymer nanoparticles,[9] use of additives,[10,11] by silanization,[12] and enzyme-based stabilizers.[13] We recently reported that enzyme–PAA conjugates added attractive features to the enzymes such as proteases (trypsin) and inhibitor (Cu^{2+}) resistance, which rendered them stable at 85–90 °C and improved shelf life (10 weeks). In this example, PAA also helped to protect catalase, a model enzyme, against heat,

Received: May 7, 2015
Revised: July 1, 2015
Published: July 8, 2015

 © 2015 American Chemical Society

DOI: 10.1021/acscatal.5b00958
ACS Catal. 2015, 5, 4979–4988

Scheme 1. Synthesis of GOx-HRP-PAA/GO Conjugate Using GOx and HRP Bienzyme and PAA and GO[a]

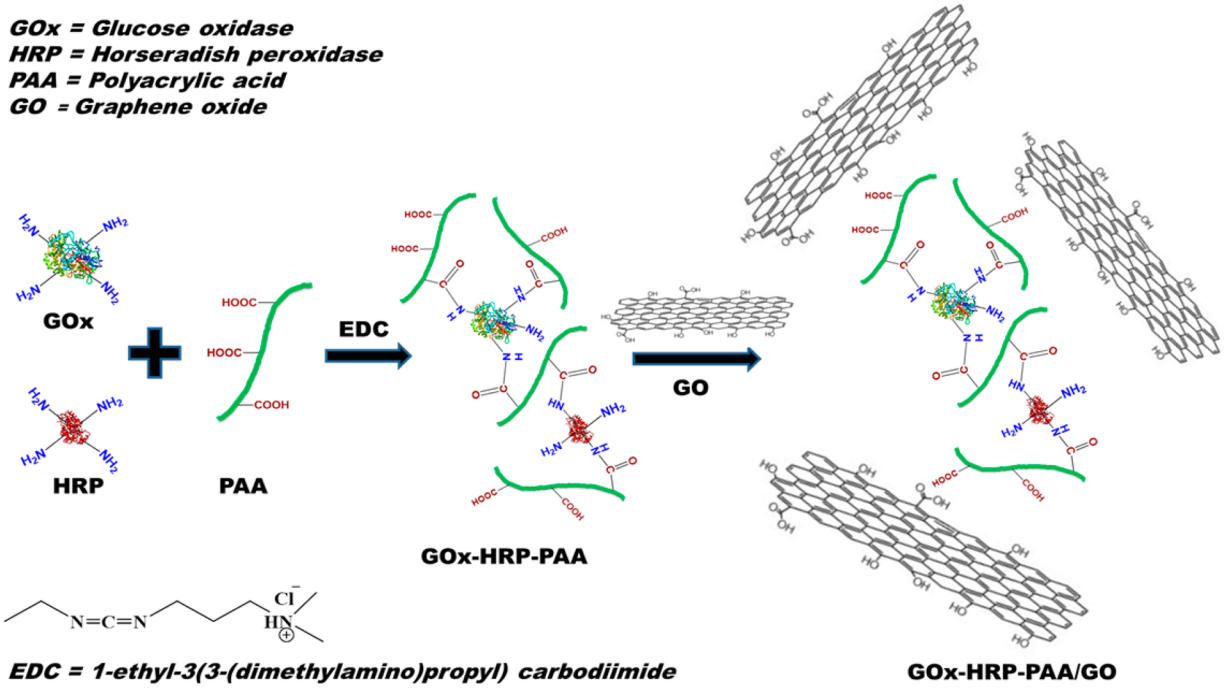

[a]HRP and GOx structures are shown above; PAA as green line and GO is represented as a sheet. EDC chemistry is used to crosslink amine groups on the enzymes with the polymer COOH groups.

inhibitors, and proteases.[14] Many examples in the literature report single-enzyme systems.[15,16] However, applications in biofuel cells and bioassay require multistep enzyme cascade reactions.[17] Thus, there is great need and substantial challenge for the stabilization of multienzyme nanobiocatalysts, which is a currently unmet challenge. Stabilized and catalytically active multienzyme nanobiocatalysts will not only enhance the productivity but will also reduce the cost of enzyme-catalyzed bioprocesses.[18]

Polymer-graphene oxide (polymer-GO) nanocomposites are a new platform to stabilize multiple enzymes on GO sheets and thus enhance their function and biological applications.[19,20] For example, GO has been conjugated covalently to polyethylene glycol, and then biologically relevant enzymes were assembled and delivered successfully to cells.[21] In another case, these types of hybrid materials were successfully used for targeted drug delivery systems where enzymes retained their structure and the biocatalyst was not released at low pH in the stomach but was released effectively at higher pH in the intestine.[22]

When enzymes were noncovalently assembled on GO, denaturation and reduced activity was noted.[23] To address these issues in our lab, an enzyme was conjugated with GO by coating its surface with sticky enzyme glues, and the enzyme activity was retained.[24] Similarly, stabilization of enzymes at high temperatures and in organic solvents was attained by intercalating enzymes between the layers of zirconium phosphate,[25] biophilized GO or by covalent attachment to PAA.[26] However, the synergetic effect of conjugation and assembly, whereby the enzyme−polymer conjugate is further protected by GO nanosheets, is expected to further enhance the protective effects of both the host materials, and this concept has never been tested. In this report, bienzyme protection using topologically distinct host materials is tested for the first time. These unique bienzyme dual-hybrid materials could be more functional than single enzyme protected by a single host material. PAA shielded the enzymes from denaturation-induced aggregation due to charge repulsion between the polymer chains.[14] Subsequent assembly of the polymer−enzyme conjugate on GO sheets could further reduce the conformational entropy of the denatured state and thereby providing improved thermodynamic stability.[27] Note that GO can also protect the encased enzymes from inhibitors and proteases.

Bienzyme catalytic cascades are used in biosensors[28] and biocatalysis.[29] Nonetheless, stability and activity of the enzyme cascade system has been a major concern. For example, GOx and HRP were immobilized within macroporous silica foam; however, stability of the conjugate at lower pHs (<5.5) and at high temperatures have not been addressed.[30] To use GOx and HRP in cascade reactions for biofuel cell applications, the enzymes need to be stabilized to perform under a variety of pHs and temperatures. Thus, in the current work, we designed and stabilized bienzyme hybrid materials, for the first time, with topologically distinct host materials and achieved remarkable pH, chemical-denaturant, and high-temperature stability. The bienzyme conjugate and the dual-hybrid system are presented in Scheme 1, where GOx and HRP are shown and green line is represented as PAA. GOx and HRP are conjugated to PAA by EDC chemistry to form GOx-HRP-PAA conjugate, which is then assembled onto the GO sheets to form GOx-HRP-PAA/GO cascade biohybrid. The GOx-HRP-PAA/GO is viewed as a nanogel of GOx-HRP-PAA assembled onto the GO sheets. This modular concept may be extended to produce environmentally benign, biologically compatible (edible), and efficient biocatalysts for the production of energy/materials as alternatives to fossil-fuel-based energy/products.

DOI: 10.1021/acscatal.5b00958
ACS Catal. 2015, 5, 4979−4988

Chart 1. Key Properties of Glucose Oxidase (GOx) and Horseradish Peroxidase (HRP)

Enzyme	Molecular weight (kDa)	Total number of residues	Number of Lys residues
GOx 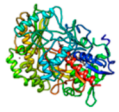	160	1166	30
HRP 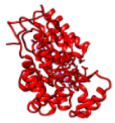	40	306	6

2. EXPERIMENTAL SECTION

2.1. Materials. PAA (M_v = 450 000 g/mol where M_v indicated viscosity average molecular weight), GOx, hydrogen peroxide (H_2O_2), *o*-methoxyphenol, EDC, sodium dodecyl sulfate (SDS), H_2SO_4, HCl, $KMnO_4$, uranyl acetate, and graphite were purchased from Sigma-Aldrich (St. Louis, MO). HRP was purchased from Calzyme Laboratories, Inc. (San Luis Obispo, CA). Agarose was purchased from Molecular Biology Hoefer, Inc. (Allison, MA).

2.2. Synthesis of GO. Graphene oxide was prepared from graphite using a modified Hummers method.[31] Graphite (1.0 g) was dispersed in concd H_2SO_4 (30 mL) and placed in an ice bath, and $KMnO_4$ (3.0 g) was added in portions with constant stirring. This mixture was heated to 50 °C for 3 h followed by addition of 70 mL of distilled water to quench the reaction. After 15 min, another 300 mL of distilled water and 30% H_2O_2 (20 mL) was added, and the color changed to bright yellow. The mixture was initially washed with 10% HCl for three times followed by washing with distilled water until neutral pH was attained. The resulting graphitic oxide powder was sonicated in buffer solution (10 mM Sodium phosphate at pH 7.0) for 45 min and centrifuged (4000 rpm for 1 h) to remove any unexfoliated graphite. GO was characterized using Raman spectroscopy, XRD, and zeta potential studies, as previously reported.[24] The supernatant solution was used for further studies. Key properties of GOx[32] and HRP[33] are shown in Chart 1.

2.3. Synthesis of Bienzyme−PAA and Bienzyme−PAA/GO Conjugates. PAA stock solution (2.8 mL, 2 wt %) was added to 1.7 mL of EDC (130 mg/mL) in 10 mM, pH 7.4 PB such that the mole ratio of −COOH of PAA and EDC was maintained at 1:1.5. GOx (800 μL, 15 mg/mL) and HRP (540 μL, 6 mg/mL) were added dropwise and stirred for 6 h. The conjugation was achieved by covalent attachment of −COOH's of PAA and Lys residues from GOx and HRP (number of Lys residues are given in Chart 1 for GOx and HRP). This conjugate is referred as GOx-HRP-PAA. Similarly, the conjugate was synthesized with GOx, without HRP, and labeled as GOx-PAA. GOx-HRP-PAA was adsorbed onto GO (0.7 mg/mL) such that weight ratio of total enzyme to GO was 1:1.5 and 1:2. These conjugates then are labeled as GOx-HRP-PAA/GO(1:1.5) and GOx-HRP-PAA/GO(1:2), respectively. All conjugates were dialyzed against PB pH 7.4 for 6 h for three cycles to remove any unreacted EDC or byproduct formed after coupling using a 8 kDa membrane. Please refer to Supporting Information for further experimental details.

3. RESULTS

In this study, GOx and HRP were conjugated to PAA together covalently and then adsorbed on to GO using noncovalent interactions resulting in bienzyme conjugate hybrids. GOx and HRP were physically mixed together using only noncovalent interactions and labeled as GOx/HRP. For comparison with the bienzyme system, several control samples were also synthesized. Synthesis of the conjugates is discussed briefly here.

3.1. Synthesis. To synthesize GOx-HRP-PAA (bienzyme conjugate) and GOx-PAA (single-enzyme conjugate), EDC chemistry was used and all the syntheses were carried out in pH 7.4 phosphate buffer. In the case of GOx-PAA and GOx-HRP-PAA, the total enzymes to PAA mole ratio was maintained at 1.2:1. The effect of GO in controlling the enzymatic activity of GOx was assayed at increasing concentrations of GO (mass percent) in the composite from 0% to 31% (7 points), indicating optimum relative specific activity (~120%) at higher GO concentrations (SI, Figure S1). Thus, in this study, we followed the optimized mass percent of GO (25 and 31%) in all the hybrids. Final mass composition of all individual components (in about 100 mg scale) is presented in Table 1. Agarose gel electrophoresis and zeta potential studies were carried out after removing excess reagents by dialysis (25 kDa cellulose membrane) for three times for 6 h each and used to

Table 1. Different Conjugates and the Mass Percent of Enzymes, PAA, and GO Used for Synthesis

samples	mass percent				description
	GOx	HRP	PAA	GO	
GOx-HRP-PAA/GO(1:1.5)	13	3.3	58	25	bienzyme conjugate hybrids
GOx-HRP-PAA/GO(1:2)	12	3.0	54	31	
GOx-HRP-PAA	18	4.5	78	0	bienzyme conjugate
GOx-PAA/GO(1:1.5)	17	0	58	25	single-enzyme conjugate hybrids
GOx-PAA/GO(1:2)	15	0	54	31	
GOx-PAA	22	0	78	0	single-enzyme conjugate
GOx/HRP	80	20	0	0	unbound bienzyme

DOI: 10.1021/acscatal.5b00958
ACS Catal. 2015, 5, 4979−4988

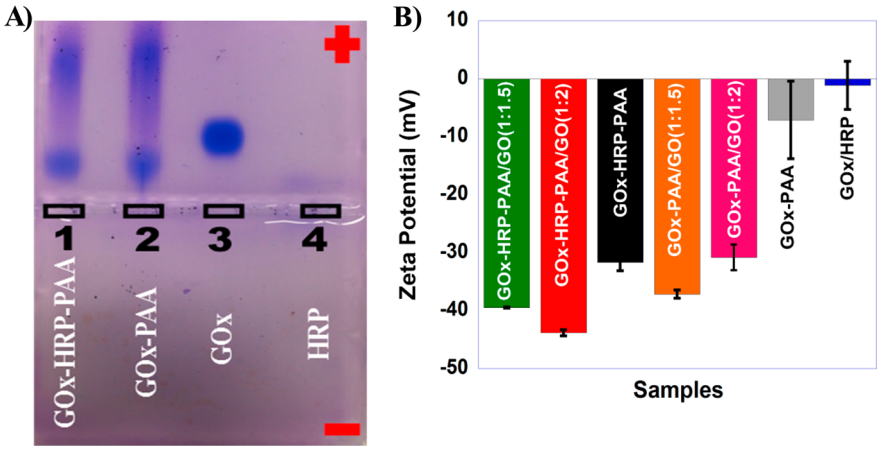

Figure 1. (A) Agarose gel electrophoresis with GOx-HRP-PAA loaded in lane 1, GOx-PAA in lane 2, GOx in lane 3, and HRP in lane 4. Agarose gel electrophoresis was done at pH 6.0, 40 mM Tris acetate buffer. HRP did not get stained well due to a mixture of enzymes which smeared in the lane. (B) Zeta potential of GOx-HRP-PAA/GO (1:1.5) (green), GOx-HRP-PAA/GO (1:2) (red), GOx-HRP-PAA (black), GOx-PAA/GO (1:1.5) (brown), GOx-PAA/GO (1:2) (pink), GOx-PAA (gray), and GOx/HRP (blue) were done at 25 °C. All measurements were performed in 10 mM sodium phosphate buffer at pH 7.0.

confirm the conjugation of the PAA and GO to enzyme and enzymes−PAA conjugate, respectively. The data is presented below.

3.2. Agarose Gel Electrophoresis. Conjugation of PAA to the enzymes and further adsorption to GO was characterized using agarose gel electrophoresis. Covalent conjugation of GOx and/or HRP to PAA was confirmed using agarose gel electrophoresis. The agarose gel is shown in Figure 1A. Lane 1 was loaded with GOx-HRP-PAA, lane 2 with GOx-PAA, lane 3 with GOx, and lane 4 with HRP. The covalent conjugation of PAA to enzymes should increase the negative charge on conjugates and ultimately increase the electrophoretic mobilities. Conversely, increase in molecular size as a result of polymer conjugation decreases the mobility of the conjugates, and thus, streaking rather than discrete entities in case of GOx-HRP-PAA and GOx-PAA was noted. This suggests the formation of enzymes−polymer nanogels[26] with variable molecular weight. HRP was not observed in the gel due to its isoenzyme features with isoelectric points ranging from 3.0 to 9.0.[34] This resulted in HRP spreading to both sides of the agarose gel and was invisible after staining. Control experiments with GOx/PAA and GOx/HRP/PAA, physical mixtures and single and bienzyme conjugate hybrids (1:2), and the agarose gel electrophoresis are displayed in Figure S2A in SI. The physical mixtures did not show any mobility relative to GOx. GOx-HRP-PAA/GO conjugates showed similar mobility as GOx-HRP-PAA, indicating noncovalent conjugation of GOx-HRP-PAA to GO.

3.3. Zeta Potential Studies. Successful modification of enzymes by PAA and adsorption onto GO was followed in solution phase using zeta potential measurements. The charge and electrophoretic motilities before and after conjugation was established by zeta potential measurements, Figure 1B. Conjugation of enzyme(s) to PAA covalently (single and bienzyme conjugates) and GO noncovalently (single and bienzyme conjugate hybrids) should result in increased negative charge on the conjugate due to −COOH groups present on PAA and GO. At pH 7.0, zeta potential of bienzyme (−1.1 mV, blue bar) decreased drastically when conjugated to PAA (bienzyme conjugate), and this can be attributed to free −COOH (pK_a = 4.2)[35] groups present on PAA (−31.7 mV, black bar). Further physical modification with GO was confirmed as the zeta potential dropped down to −39.5 mV (green) and −43.8 mV (red) for bienzyme conjugate hybrids with (1:1.5) and (1:2) ratio of total enzymes to GO (w/w), respectively. Similar results were also noted in the case of single-enzyme conjugates where zeta potential of −7.1 mV (GOx-PAA) (gray) was dropped to −37.2 (orange) and −30.8 mV (pink), respectively, for single-enzyme conjugate hybrids with ratio of (1:1.5) and (1:2). Zeta potential of PAA and GO was found to be −46.0 and −37.9 mV, respectively (Figure S2B in SI).

3.4. Circular Dichroism (CD) Studies. The change in enzymes' secondary structure after each modification was examined using far-UV circular dichroism (CD) studies. The secondary structures and relative % ellipticity of the bienzyme, PAA conjugates, GO conjugates, and conjugate hybrids were analyzed using far-UV CD studies. It is expected that after conjugation with PAA and GO, GOx/HRP or GOx was supposed to lose its relative % ellipticity due to the strain imposed on its secondary structure from covalent conjugation with PAA and noncovalent conjugation with GO.[24] Figure 2 presents the comparison of the percent retention of the ellipticity of bienzyme and that of their respective PAA and/or GO conjugates. These studies were carried out in PB pH 7.4, 10 mM buffer; in this figure, ellipticity at 222 nm of GOx/HRP is referenced as 100%. The CD spectra of the unmodified bienzyme, single and bienzyme conjugates, and corresponding GO conjugate hybrids, bare GO, and PAA are shown in Figure S3 in SI. Spectra of bare GO and PAA confirm absence of scattering and structure from these samples (Figure S3, SI).

From Figure 2, conjugation of PAA to the enzymes resulted in decreased % ellipticity retention. The blue bar in Figure 2 indicates unmodified GOx/HRP, which is referenced to 100% CD ellipticity retention. GOx-HRP-PAA/GO (1:1.5) (green bar) and (1:2) (red bar) presented 87% and 94% ellipticity retention, and GOx-PAA/GO (1:1.5) (orange bar) and (1:2) (pink bar) showed 71% and 78% of the same. This % ellipticity of the single and bienzyme conjugate hybrids was lower than single or bienzyme conjugate counterparts. GOx-HRP-PAA (black bar) showed 94% and GOx-PAA (gray bar) showed 73% ellipticity retention. Also, the presence of Fe in HRP soret

DOI: 10.1021/acscatal.5b00958
ACS Catal. 2015, 5, 4979−4988

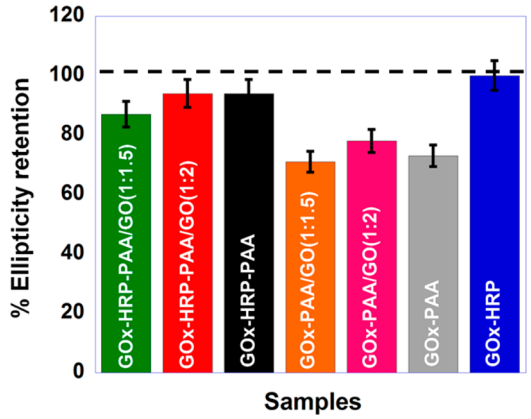

Figure 2. Comparison of the CD secondary structure retention in PB pH 7.4, 10 mM of GOx-HRP-PAA/GO(1:1.5) (green), GOx-HRP-PAA/GO(1:2) (red), GOx-HRP-PAA (black), GOx-PAA/GO(1:1.5) (orange), GOx-PAA/GO(1:2) (pink), GOx-PAA (gray), and GOx/HRP (blue). Ellipticity at 222 nm in mdeg/μM·cm is used to calculate % ellipticity retention and ellipticity at 222 nm of GOx/HRP is referenced at 100 nm.

environment and inside PAA conjugate was confirmed using optical spectroscopy. For example, GOx-HRP-PAA and native HRP showed a peak at ∼403 nm, confirming the same. The samples were dialyzed to remove any free HRP using a membrane with a cutoff size of 25 kDa. The plot can be found in SI Figure S4 (concentration of HRP was normalized to 2 μM). Soret optical spectra for bienzyme conjugate hybrid showed extensive scattering due to GO and are not provided.

3.4. Transmission Electron Microscopy (TEM). Morphology of collapsed structure of GOx-HRP-PAA/GO (1:2), GOx-HRP-PAA, and GOx/HRP conjugates was examined using TEM. As seen from Figure 3A, micrograph of GOx-HRP-PAA/GO (1:2) showed cross-linked enzymes polymer networks assembled on graphene basal plane. Figure 3B showed nanogel morphology for GOx-HRP-PAA, whereas Figure 3C displayed aggregated enzyme particles of GOx/HRP. TEM micrograph of bare GO, Figure S5 in SI, displayed smoother texture compared to GOx-HRP-PAA/GO (1:2). This suggests successful physical adsorption of GOx-HRP-PAA nanogel onto GO.

3.5. Activity Studies. GOx has a narrow range of optimal pH (pH 5−6), and HRP has optimal pH of 4.2 at which these enzymes show enzymatic activity.[7,8] The catalytic activity studies of single and bienzyme conjugates, hybrids, and unmodified bienzyme were examined at biologically challenging conditions of pH (2.5−7.4), temperature (25 and 65 °C), and denaturant concentration (4 mM of surfactants). Oxidase activity of GOx was monitored using glucose as a substrate.[36] Relative specific activity was calculated for each sample by using the initial rate of unmodified GOx activity at 25 °C in pH 7.4 phosphate buffer. These hybrid systems showed exceptional stability at diverse conditions, whereas unmodified enzymes showed negligible activity. In the case of single-enzyme conjugates and hybrids, HRP was added at the time of activity measurements and used as controls for comparison only.

3.5.1. Activity Studies at Room Temperature and pH 7.4. Benchmark activity measurements were performed using unbound bienzyme, conjugates, and hybrids at room temperature and at pH 7.4. Under these conditions, GOx/HRP specific activity was referenced to 100%, and this was used to standardize specific activities of all other samples, Figure 4A. The kinetic plots of all the conjugates and hybrids as well as GOx/HRP are presented in Figure S6 in SI. Accordingly, GOx-HRP-PAA/GO(1:1.5), GOx-HRP-PAA/GO(1:2) and GOx-HRP-PAA, showed 144, 157 and 141% activities, respectively. Evidently, % specific activity of the PAA and subsequent GO conjugated to GOx/HRP were very high. This observation led us to investigate the robustness of our conjugates under severe conditions for a wide range of applications, as discussed in the next few sections.

3.5.2. Activity Studies at Different pH Values in Presence and Absence of a Chemical Denaturant. The pH profile of the enzymatic activity of the biohybrids was tested in the presence of SDS, a denaturant, which reduces the activity of the enzymes. Catalytic activities were established at pH 2.5, 4.0, 5.5, and 7.4 with and without SDS (4 mM).

From Figure 4A, bienzyme conjugate hybrids activities were 85−95% at pH 2.5, 4.0, and 5.5 except in the case of GOx-HRP-PAA/GO(1:2) at pH 2.5 where it showed high activity of 124%. In the case of GOx-HRP-PAA, retained activity at pH 2.5 was 78%, which was more than the activity at pH 4.0 and 5.5 (∼60%). Bienzyme showed 14% retention in activity at pH 2.5, which increased with pH and was 100% at pH 7.4. In the presence of 4.0 mM SDS (Figure 4B), GOx-HRP-PAA and GOx-HRP-PAA/GO (1:1.5) and (1:2) conjugates and conjugate hybrids showed 47, 90, and 84% specific activities at pH 5.5, respectively. The highest activity was observed with GOx-HRP-PAA/GO (1:2) with or without SDS. At pH 5.5, single-enzyme conjugates and hybrids, GOx-PAA and GOx-

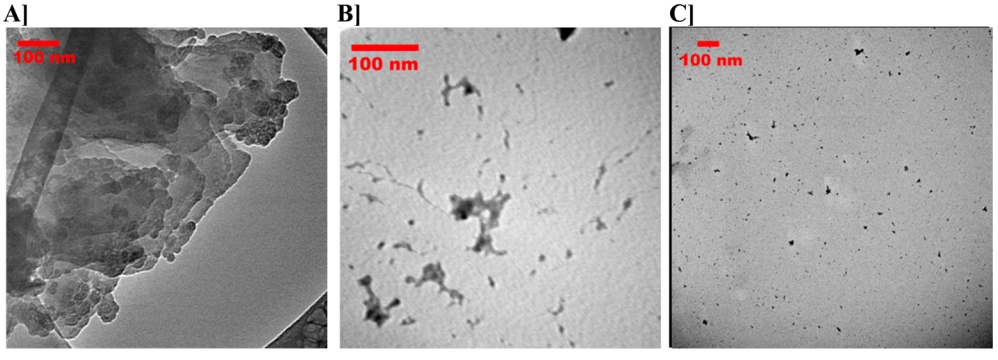

Figure 3. TEM micrographs of (A) GOx-HRP-PAA/GO (1:2), (B) GOx-HRP-PAA, and (C) GOx/HRP. All samples were stained with 0.5% w/w uranyl acetate. GOx-HRP-PAA/GO (1:2) showed nanogels assembled on GO sheets, GOx-HRP-PAA showed nanogels, and GOx/HRP showed aggregated particles.

DOI: 10.1021/acscatal.5b00958
ACS Catal. 2015, 5, 4979−4988

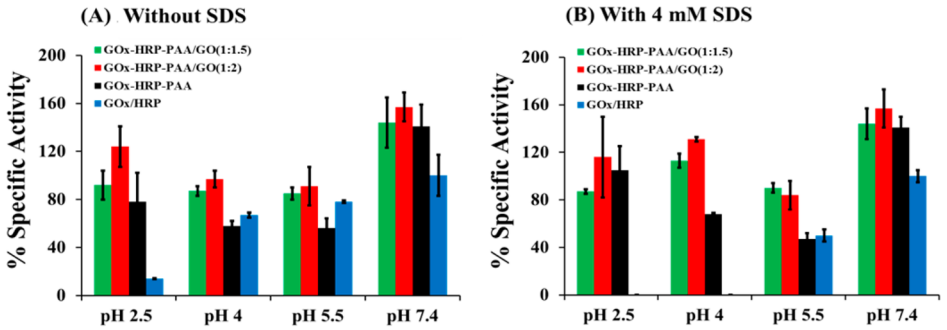

Figure 4. (A) Activity study as a function of increasing pH without SDS. (B) Activity study at increasing pHs with 4.0 mM SDS (denaturant) – GOx-HRP-PAA/GO (1:1.5) (green), GOx-HRP-PAA/GO (1:2) (red), GOx-HRP-PAA (black,) and GOx/HRP (blue). Activity of single-enzyme GOx-PAA and GOx-PAA/GO (1:1.5) and (1:2) is presented inSI Figure S7. Initial activity of each sample (20–40 s) was measured and compared to GOx/HRP, which was referenced to 100%.

PAA/GO, showed comparable activities to bienzyme conjugate hybrids (Figure S7, SI). In sharp contrast, with 4.0 mM SDS and at lower pHs (2.5 and 4.0), unbound bienzyme showed negligible activity. At pH 7.4, the bienzyme showed 100% activity, which was double of its activity at pH 5.5 (50%).

We tested the recyclability of GOx-HRP-PAA/GO (1:2) and GOx-PAA/GO (1:2). Single-enzyme conjugate hybrid failed to show any recyclability, whereas bienzyme conjugate hybrid (GOx-HRP-PAA/GO (1:2)) showed recyclability up to two cycles in pH 2.5 and up to three cycles in pH 7.4 in the absence of SDS. When recyclability studies were performed in the presence of 4 mM SDS, the bienzyme conjugate hybrid showed recyclability up to only one cycle at pH 2.5 and 7.4. Corresponding activity at each cycle can be found in Figure S8 in SI.

3.5.3. Activity Studies at 65 °C. The optimal temperature for catalytic activity of GOx is ~60 °C.[2] Therefore, activity studies were performed at 65 °C to test the robustness and effectiveness of the bienzyme conjugates and hybrids and to evaluate the impact of GO on thermal stability of the conjugates. Figure 5 summarized the activity study plot of the GOx/HRP bienzyme and other conjugates and hybrids. The activity retention was calculated by using the initial rate of free bienzyme at 25 °C as the reference (100%). GOx-HRP-PAA/GO showed ~120% activity, which was 40% higher than single-enzyme conjugate as well as hybrids. GOx-PAA/GO conjugate hybrids showed 70–80% activity. GOx/HRP showed ~12% activity, whereas bienzyme and single-enzyme conjugates retained 60–80% activity.

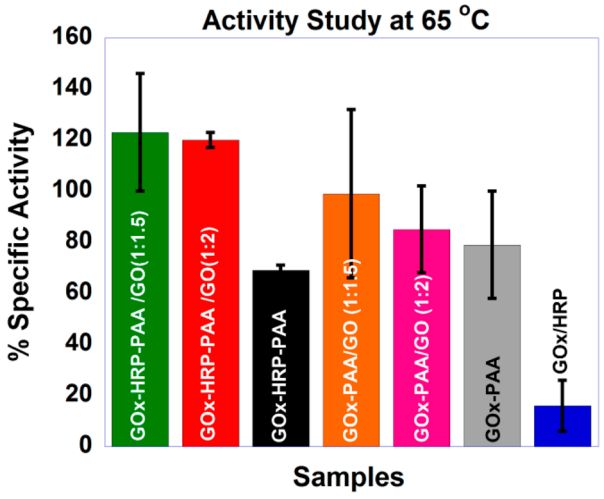

Figure 5. Activity study at 65 °C for dual and single enzyme systems. % Specific activity of GOx-HRP-PAA/GO(1:1.5) (green), GOx-HRP-PAA/GO (1:2) (red), GOx-HRP-PAA (black), GOx-PAA/GO(1:1.5) (orange), GOx-PAA/GO (1:2) (pink), GOxPAA (gray), and GOx/HRP (blue) were compared to 100% specific activity of GOx/HRP at room temperature and pH 7.4.

To test the robustness of the bienzyme conjugate hybrid, recyclability studies were performed at 65 °C in pH 7.4 using GOx-HRP-PAA/GO (1:2). It showed recyclability up to one cycle. The recyclability study graph can be found in Figure S9 in SI.

3.6. Kinetics Studies. The enzymatic catalytic rates were computed using Lineweaver–Burk plots, which were assembled by plotting 1/initial rate versus 1/substrate concentration, and Michaelis–Menten constant (K_M) and maximum catalytic rate (V_{max}) were calculated. The inverse of the *Y*-intercept and negative inverse of *X*-intercept of the Lineweaver–Burk plot were used to determine the V_{max} and K_M, respectively. Higher K_M indicates lower affinity of the substrate toward the enzyme and vice versa. These studies helped investigate the catalytic efficiency and K_{cat} (catalytic rate constant) of each system. In the case of biological catalysts such as enzymes and modified enzymes, catalytic turnover numbers are presented in terms of K_{cat} values.[37] In these studies, increasing amounts of glucose were used, and initial rates were calculated. Lineweaver–Burk plots (GOx-HRP-PAA/GO(1:2), GOx-PAA/GO(1:2), GOx-HRP-PAA, GOx-PAA, and GOx/HRP) are shown in Figure S10 in SI. The corresponding K_M, V_{max}, K_{cat} (turnover numbers) and K_{cat}/K_M (catalytic efficiency) are presented in Table S1 in SI.

Three-dimensional plots of catalytic efficiency and K_{cat} of all the conjugates are presented in Figure 6. Kinetic plots of GOx-HRP-PAA/GO(1:1.5) and GOx-PAA/GO(1:1.5) were not computed because conjugate hybrids, GOx-HRP-PAA/GO(1:2), and GOx-PAA/GO(1:2) showed better catalytic activity at higher temperature and lower pHs. GOx-HRP-PAA showed the highest K_{cat} of 69×10^{-2} s^{-1} followed by GOx-HRP-PAA/GO(1:2), GOx-PAA, GOx-PAA/GO(1:2), and GOx-HRP with values of 68×10^{-2}, 68×10^{-2}, 57×10^{-2}, and 32×10^{-2} s^{-1} respectively. In the case of catalytic efficiency, GOx-HRP-PAA/GO(1:2) showed the highest of 69 mM^{-1} s^{-1}, and GOx-HRP-PAA showed the lowest of 47 mM^{-1} s^{-1}. GOx/HRP, GOx-PAA, and GOx-PAA/GO (1:2) had catalytic efficiency of 59, 63, and 63 mM^{-1} s^{-1} respectively. In Table S1 in SI, K_M and V_{max} are presented. K_M values indicate

DOI: 10.1021/acscatal.5b00958
ACS Catal. 2015, 5, 4979–4988

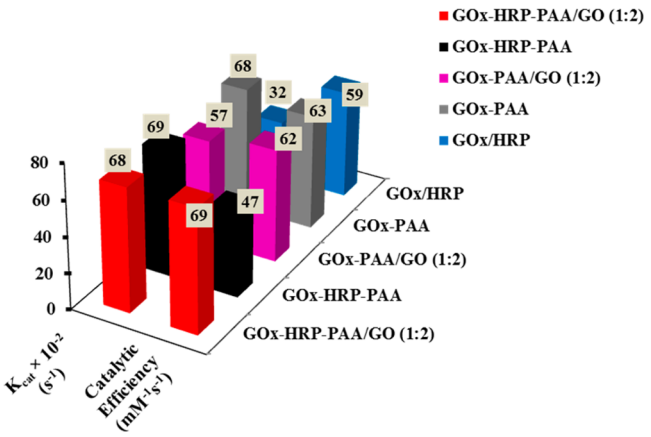

Figure 6. Catalytic efficiency and K_{cat} of GOx-HRP-PAA/GO(1:2) (red), GOx-HRP-PAA(black), GOx-PAA/GO(1:2) (pink), GOx-PAA (gray), and GOx/HRP (blue) in PB pH 7.4 and 10 mM with enzyme concentration of 0.5 μM, varying glucose (0.075 mM- 0.6 mM), and *o*-methoxyphenol (1.125 mM).

the affinity toward the substrate. The lower K_M value, the higher the affinity, and vice versa. GOx/HRP showed the lowest K_M and V_{max} of 0.55 mM and 0.016 μM^{-1} s^{-1} respectively, whereas GOx-HRP-PAA showed the highest K_M and V_{max} values of 1.46 mM and 0.035 μM^{-1} s^{-1}, respectively. However, K_M and K_{cat} values of GOx reported elsewhere were 1.34 mM[38] and 16 × 10^{-2} s^{-1},[39] respectively, which was very different from our values (0.55 mM and 32 × 10^{-2} s^{-1}), and this is to be expected for cascade catalysis. The diffusional characteristics of substrates for free enzymes versus bound enzymes are responsible for these differences.

4. DISCUSSION

Here, GOx and HRP are modified by covalent attachment with PAA using EDC chemistry and subsequently adsorbed on GO to prepare highly stable quaternary hybrid biocatalysts of GOx-HRP-PAA/GO. Synergetic effect from the host materials, which are capable of enhancing enzymes' thermodynamic stability, has bestowed substrate channeling between the enzymes and thermal and chemical stability at various denaturing conditions. GO nanolayers with oxygen functional groups showed affinity with PAA by H-bonding interactions.[22] We have demonstrated that PAA conjugation is highly effective in protecting enzymes from various stresses like temperature, aggregation and proteases.[14] For example, catalase−PAA conjugates were thermally stable at ∼90 °C, and the same conjugates improved the shelf life of catalase by 8 weeks at 8 °C.[14] Going forward, we wish to investigate the stability enhancement of multienzyme polymer conjugate by employing another host material. We also wish to explore if it is possible to render these multienzymes polymer conjugates more functional by the presence of another host matrix. We demonstrate a general approach combining conjugation and assembly for design of the enzymes−polymer hybrids on solid supports for catalytic applications. The catalytic properties presented by these hybrid materials cannot be realized from just simple enzymes−polymer conjugates or physical mixtures.

Successful syntheses of single and bienzyme conjugates and hybrids were verified using agarose gel electrophoresis, TEM, and zeta potential studies. Covalent conjugation of enzymes with PAA was confirmed using agarose gel at pH 6.0. The presence of −COOH groups in PAA imparted more negative charges to the conjugates compared to unmodified enzymes, and thus, the PAA conjugates showed ∼120% more mobility as compared to GOx. The streaking bands from enzymes−polymer conjugates resulted from polydisperse PAA−enzyme nanogel formation. These observations in agarose gels were corroborated by observations from zeta potential studies as well. TEM images of collapsed GOx-HRP-PAA/GO (1:2) showed assembly of nanogels of GOx-HRP-PAA onto GO sheets (Figure 3A and 3B, respectively), whereas GOx/HRP showed aggregated particles (Figure 3C). Nanogel formation of GOx/HRP when conjugated to PAA was expected, as we have previously observed nanogels from single-enzyme conjugation to PAA.[23]

Zeta potential is a handy tool to monitor electrostatic changes around negatively charged GO basal plane at successive steps.[24] The zeta potential of single and bienzyme conjugate and hybrids are dictated by PAA and/or GO because of their large size compared to single-enzymes molecule. The interaction of enzyme conjugates with GO did not result in a big shift of surface potential, which indicated that electrostatic interactions are less dominant leading us to believe that most of the amino groups in the surface of the enzymes are modified by PAA. In this scenario, a possible driving force is the hydrogen bonding between carboxyl/amide groups of enzymes−PAA conjugates and oxygen-based functional groups at the GO interface.[22]

CD study was carried out to investigate the effect of polymer conjugation and subsequent immobilization onto GO on the secondary structure of the enzyme, which is vital for biological function and its biocatalytic activity. Conjugation with PAA and further adsorption to GO resulted in some secondary structural changes to the enzymes, as the maximum of 30% ellipticity loss was noted (Figure 2). The reduction in the ellipticity could be attributed to the unfavorable hydrophobic interaction of the enzymes interior with GO. Despite these adverse interactions, enzymes within PAA and GO matrix may still be protected and retain some secondary structure.[24] More importantly, catalytic activity determination suggests that enzymatic activity of the biocatalysts is not compromised due to perceived structural denaturation. This was verified by extensive catalytic activity measurements carried out at different pH, with and without denaturant (4.0 mM SDS), and at high temperature (65 °C) with a variety of samples and controls.

Although thermal stability and shelf life of different enzyme−polymer conjugates are well documented, stability of enzymes against denaturants and at low pHs are poorly understood. We discovered that some enzymes may be protected from acid denaturation by conjugating with PAA. For example, GOx-HRP-PAA conjugate showed nearly 80% activity at pH 2.5, whereas GOx/HRP had negligible activity (∼14%) under similar conditions. This indicates that both GOx and HRP are stabilized within PAA due to the marginal reduction of the conformational entropy of the denatured state of the enzyme(s) compared to the unmodified enzyme(s).[27] This is the first example of enzymes(s)−polymer conjugates, wherein two enzymes were stabilized simultaneously within a single polymer network.

In GOx-HRP-PAA/GO, improvement in stabilization may be due to the presence of GO layers[40] despite diffusional limitation of the substrate and the products. Interestingly, immobilization of GOx-HRP-PAA onto GO resulted in remarkable quantitative retention (100%) in catalytic activities over a broad pH range. Thus, despite loss of % ellipticity from CD studies, minor

DOI: 10.1021/acscatal.5b00958
ACS Catal. 2015, 5, 4979−4988

Table 2. Comparison of Substrate Channeling Efficiency of Current Catalytic System with Other Relevant Reports

no.	enzymes used in multienzyme systems	degree of substrate channeling	temperature of the study	pH of the study	concn of surfactant (SDS) (mM)
1	Krebs cycle enzymes[47]	1−2	25	7−8	not applicable (NA)
2	ferredoxin and hydrogenase[48]	1	25	7−8	NA
3	GOx and HRP[49]	20−30	25	7−8	NA
4	cellulosomes[50]	2−4	37	6−7	NA
5	tryptophan synthase[51]	infinite	25	6−7	NA
6	**this work (GOx and HRP)**	**1.3**	**25**	**7.4**	**4.0**
7	**this work (GOx and HRP)**	**infinite**	**25**	**2.5**	**4.0**
8	**this work (GOx and HRP)**	**7.5**	**65**	**7.4**	**NA**

structure deformation can improve the enzymatic activity by improved access to the active sites.[24] TEM of GOx and HRP conjugated to PAA and assembled onto GO clearly showed the successful decoration of enzymes polymer conjugates in the GO layers. This supports the above hypothesis that GO is acting as another shield against various stresses like pH and SDS.

GOx is a very robust enzyme, and its SDS denaturation is possible only at lower pH values (~3.0).[41] Also, under similar low pH conditions, HRP is enzymatically deactivated.[42,43] Here, a modular approach is shown to stabilize the pH profile of GOx as well as HRP with SDS. Polymer sheath of PAA around enzymes stabilizes them from thermal denaturation, as shown previously.[46] However, stability to chemical denaturants like SDS has never been addressed before. At pH 2.5−7.4 with SDS, these bienzyme conjugates and hybrids indicated high activities compared to single-enzyme counterparts or unmodified bienzyme system. Only at pH 5.5 have single-enzyme conjugate hybrids showed comparable activities to bienzyme conjugate hybrids. These results indicate that PAA is a good candidate to induce denaturant resistivity to the enzymes as SDS showed hydrophobic binding with PAA with favorable enthalpy and entropic contributions.[44] PAA conjugation could also alter the pK_a of the active site by shielding from the bulk and could thereby be responsible for retention of activity, but experimental access to such information may not be easy. Furthermore, PAA conjugation has improved not only the stability of the enzymes against SDS but also the stability of enzymes at low pH conditions. Negatively charged COOH groups of PAA act as an electrostatic repulsion barrier for SDS-like anionic surfactant to get access to the enzyme surface in order to unfold the molecule. In addition, GO sheets further enhanced this stability despite diffusional problem of the substrates in the presence of multiple GO layers around the enzyme(s). GO can also interact with SDS, which in turn results in reduced interaction of SDS toward enzymes.[45] These factors may help in stabilizing the enzymes against high concentration of the denaturant.

We mentioned previously that some of our conjugates displayed activities higher than 100%, which has been attributed to substrate channeling across the matrix. Despite diffusional limitation of the substrate and the products across GO and PAA matrix, H_2O_2 (a product of GOx reaction and substrate for HRP reaction) is able to internally diffuse within the matrix. This effect might help overcome problems of bulk diffusion to the matrix affording high initial catalytic rates of reactions. Furthermore, this robust bienzyme conjugate and hybrid platform may be exploited for high temperature enzyme catalysis with substrate channeling.

To determine thermal stability of conjugates, catalytic activities were established at 65 °C and compared to appropriate control samples. For example, GOx is inactive above 50 °C, and HRP presents reduced activity (65%) at 42 °C.[2,6] However, when GOx (and HRP) was conjugated with PAA, it seemed to have regained some of the activity (60−80%) because the conformational entropy of the denatured state is reduced as result of PAA confinement. Therefore, the heat of denaturation of enzyme increases,[46] and the enzyme is stabilized more than its unmodified counterparts. This stabilization is enhanced when the PAA-conjugated GOx (and HRP) are adsorbed onto GO as a consequence of further reduction in entropy and possibly due to elevated substrate channeling. This is proved by the activity data shown in Figure 6, wherein GOx-HRP-PAA/GO and GOx-PAA/GO showed higher % specific activity retention compared to single and bienzyme conjugated samples (GOx-HRP-PAA/GOx-PAA). Additionally, at high temperatures, the rate of the reaction can increase by several fold in accordance with the Arrhenius equation. Conversely, H_2O_2 decomposition at elevated temperatures may be an opposing effect to the above two. However, in our conjugates, both donor and acceptor enzymes are in a close proximity so that H_2O_2 transfer becomes internally very efficient prior to the decomposition step. This is, again, a very rare example of enzymes cascading with high retention of activity at thermally denaturing conditions.

To better understand and compare the effectiveness of the substrate channeling of current system, we computed the degree of substrate channeling (DSC). DSC is calculated by using the ratio of initial rate of the bienzyme conjugate hybrids (1:2) system to that of the bienzyme alone under comparable conditions. These DSC values are then compared to the few relevant examples of multienzyme systems published in literature[47−51] and are presented in Table 2.[17] To our best knowledge, only the current system demonstrated active substrate channeling at diverse conditions including high temperature and with denaturant of 4.0 mM. Thus, effective substrate channeling can be achieved using PAA in conjunction with GO.

Kinetic data showed that adsorption of GOx-HRP-PAA to GO increases the catalytic efficiency of the GOx/HRP (unmodified bienzyme) system. Also, the highest K_{cat} of the GOx-HRP-PAA showed the importance of bienzyme conjugation instead of single-enzyme conjugation. Furthermore, high catalytic efficiency of GOx-HRP-PAA/GO (1:2) may be due to the presence of PAA matrix, which is a hydrophilic polymer that aids in transport of the glucose to the catalytic site within GOx and subsequent removal of the products. This constant replenishment of substrate and further depletion of products from the enzyme active site may be responsible for the enhancement of the K_{cat} and catalytic efficiency of the bienzyme conjugates. Also, high K_M indicated the decrease in selectivity of glucose toward GOx of the GOx-HRP-PAA. This could be due

DOI: 10.1021/acscatal.5b00958
ACS Catal. 2015, 5, 4979−4988

to the change in conformation of the active site of the enzyme, which is supported by our CD data (Figure 3). This resulted in an increase in V_{max}, which may be related to the hydrophilic PAA matrix. The conclusions drawn from the kinetics studies are rudimentary and require extensive investigation.

5. CONCLUSION

This is the first example of bienzyme (HRP and GOx) stabilization using PAA and GO sheets and proof-of-concept of bienzyme cascade catalytic effects. GOx/HRP (bienzyme) and GOx were covalently modified with PAA using EDC chemistry and then assembled on GO using noncovalent interactions. These versatile bienzyme conjugates have been used to enhance: (1) stability of these enzymes under harsh conditions of pH (2.5−7.4) and denaturants (SDS); and (2) enhanced biocatalytic activities of the catalytic cascade in the dual-host system, when compared to a mixture of the two enzymes in the solution. Furthermore, the bienzyme activity improved at higher temperatures compared to their single-enzyme counterparts. This new platform bestowed stabilization of two different enzymes simultaneously to implement substrate channeling at high temperature, broad pH, and chemically denaturing conditions with retained enzymatic activity. Polymer wrapping followed by contact with GO resulted in reducing the substrate specificity of the enzymes because of loss in ellipticity retention, but the highest catalytic efficiency (K_{cat}) of GOx-HRP-PAA/GO (1:2) is obtained as a bonus. Therefore, this bienzyme composite cascade mechanism proved to be highly efficient and showed stability at high temperature, which has not been achieved by unbound enzymes or polymer conjugates. This combination of a 2D host material for a enzymes−polymer guest opens up a new platform for multienzyme cascading for broad spectrum of applications, at diverse and biologically inaccessible conditions. This is one of the first enzyme hybrids with substrate channeling demonstrated at diverse and challenging conditions. The versatility of this system to protect more than two enzymes needs to be tested, which could lead to the design of micro biofuel cells and biobatteries. Also, in the long term, this modular methodology may be used to produce environmentally benign, biocompatible, edible, and efficient biocatalysts for energy production as alternatives to fossil fuel-based energy.

■ ASSOCIATED CONTENT

Supporting Information

The Supporting Information is available free of charge on the ACS Publications website at DOI: 10.1021/acscatal.5b00958.

Experimental details and supplemental data as noted in the text (PDF)

■ AUTHOR INFORMATION

Corresponding Authors

*E-mail: challa.kumar@uconn.edu.

*E-mail: kasi@ims.uconn.edu. Phone: 860-486-4713. Fax: 860-486-4745.

Notes

The authors declare no competing financial interest.

■ ACKNOWLEDGMENTS

C.V.K. and A.P. thank NSF EAGER award (DMR-1441879). C.V.K. and R.M.K. acknowledge financial support University of Connecticut Research Foundation Research Excellence Program Award 2015. C.V.K. thanks his 9th grade science teacher for early inspiration.

■ REFERENCES

(1) Cooper, V. A.; Nicell, J. A. *Water Res.* **1996**, *30*, 954−964.

(2) Wong, C.; Wong, K.; Chen, X. *Appl. Microbiol. Biotechnol.* **2008**, *78*, 927−938.

(3) Guo, X.; Liang, B.; Jian, J.; Zhang, Y.; Ye, X. *Microchim. Acta* **2014**, *181*, 519−525.

(4) Delvaux, M.; Walcarius, A.; Demoustier-Champagne, S. *Biosens. Bioelectron.* **2005**, *20*, 1587−1594.

(5) Ramachandran, S.; Fu, E.; Lutz, B.; Yager, P. *Analyst* **2014**, *139*, 1456−1462.

(6) Lavery, C. B.; MacInnis, M. C.; MacDonald, M. J.; Williams, J. B.; Spencer, C. A.; Burke, A. A.; Irwin, D. J. G.; D'Cunha, G. B. *J. Agric. Food Chem.* **2010**, *58*, 8471−8476.

(7) Munoz-Munoz, J. L.; Garcia-Molina, F.; Varon, R.; Rodriguez-Lopez, J. N.; Garcia-Canovas, F.; Tudela, J. *Biosci., Biotechnol., Biochem.* **2007**, *71*, 390−396.

(8) Jo, S. M.; Lee, H. Y.; Kim, J. C. *Int. J. Biol. Macromol.* **2009**, *45*, 421−426.

(9) He, C.; Liu, J.; Xie, L.; Zhang, Q.; Li, C.; Gui, D.; Zhang, G.; Wu, C. *Langmuir* **2009**, *25*, 13456−13460.

(10) Gouda, M. D.; Singh, S. A.; Rao, A. G. A.; Thakur, M. S.; Karanth, N. G. *J. Biol. Chem.* **2003**, *278*, 24324−24333.

(11) Paz-Alfaro, K. J.; Ruiz-Granados, Y. G.; Uribe-Carvajal, S.; Sampedro, J. G. *J. Biotechnol.* **2009**, *141*, 130−136.

(12) Sarath Babu, V. R.; Kumar, M. A.; Karanth, N. G.; Thakur, M. S. *Biosens. Bioelectron.* **2004**, *19*, 1337−1341.

(13) Eremin, A. N.; Budnikova, L. P.; Sviridov, O. V.; Metelitsa, D. I. *Appl. Biochem. Microbiol.* **2002**, *38*, 151−158.

(14) Riccardi, C. M.; Cole, K. S.; Benson, K. R.; Ward, J. R.; Bassett, K. M.; Zhang, Y.; Zore, O. V.; Stromer, B.; Kasi, R. M.; Kumar, C. V. *Bioconjugate Chem.* **2014**, *25*, 1501−1510.

(15) Kumar, C. V.; Chaudhari, A. *J. Am. Chem. Soc.* **2000**, *122*, 830−837.

(16) Panchagnula, V.; Kumar, C. V.; Rusling, J. F. Ultrathin Layered Myoglobin−Polyion Films Functional and Stable at Acidic pH Values. *J. Am. Chem. Soc.* **2002**, *124*, 12515−12521.

(17) Zhang, Y. H. P. *Biotechnol. Adv.* **2011**, *29*, 715−725.

(18) Santacoloma, P. A.; Sin, G. r.; Gernaey, K. V.; Woodley, J. M. *Org. Process Res. Dev.* **2010**, *15*, 203−212.

(19) Wang, Y.; Li, Z.; Wang, J.; Li, J.; Lin, Y. *Trends Biotechnol.* **2011**, *29*, 205−212.

(20) Zhang, Y.; Wu, C.; Guo, S.; Zhang, J. *Nanotechnol. Rev.* **2013**, *2*, 27−45.

(21) Shen, H.; Liu, M.; He, H.; Zhang, L.; Huang, J.; Chong, Y.; Dai, J.; Zhang, Z. *ACS Appl. Mater. Interfaces* **2012**, *4*, 6317−6323.

(22) Kavitha, T.; Kang, I. K.; Park, S. Y. *Langmuir* **2013**, *30*, 402−409.

(23) Zhang, Y.; Zhang, J.; Huang, X.; Zhou, X.; Wu, H.; Guo, S. *Small* **2012**, *8*, 154−159.

(24) Pattammattel, A.; Puglia, M.; Chakraborty, S.; Deshapriya, I. K.; Dutta, P. K.; Kumar, C. V. *Langmuir* **2013**, *29*, 15643−15654.

(25) Kumar, C. V.; Chaudhari, A. *Chem. Commun.* **2002**, *20*, 2382−2383.

(26) Zore, O. V.; Lenehan, P. J.; Kumar, C. V.; Kasi, R. M. *Langmuir* **2014**, *30*, 5176−5184.

(27) Kumar, C. V.; Chaudhari, A. *Chem. Commun.* **2002**, *21*, 2382−2383.

(28) Jeykumari, D. R. S.; Narayanan, S. S. *Biosens. Bioelectron.* **2008**, *23*, 1686−1693.

(29) Rocha-Martín, J.; Rivas, B.; Muñoz, R.; Guisán, J. M.; López-Gallego, F. *ChemCatChem* **2012**, *4*, 1279−1288.

(30) Cao, X.; Li, Y.; Zhang, Z.; Yu, J.; Qian, J.; Liu, S. *Analyst* **2012**, *137*, 5785−5791.

(31) Hummers, W. S.; Offeman, R. E. *J. Am. Chem. Soc.* **1958**, *80*, 1339−1339.

DOI: 10.1021/acscatal.5b00958
ACS Catal. 2015, 5, 4979−4988

(32) Carlsson, G. H.; Nicholls, P.; Svistunenko, D.; Berglund, G. I.; Hajdu, J. *Biochemistry* **2005**, *44*, 635−642.
(33) Kommoju, P. R.; Chen, Z. W.; Bruckner, R. C.; Mathews, F. S.; Jorns, M. S. *Biochemistry* **2011**, *50*, 5521−5534.
(34) Fieldes, M. A. *Electrophoresis* **1992**, *13*, 82−86.
(35) Liu, Y.; Wang, W.; Jin, Y.; Wang, A. *Sep. Sci. Technol.* **2011**, *46*, 858−868.
(36) Gibson, Q. H.; Swoboda, B. E. P.; Massey, V. *J. Biol. Chem.* **1964**, *239*, 3927−3934.
(37) Axley, M. J.; Bock, A.; Stadtman, T. C. *Proc. Natl. Acad. Sci. U. S. A.* **1991**, *88*, 8450−8454.
(38) Shin, K. S.; Youn, H. D.; Han, Y. H.; Kang, S. O.; Hah, Y. C. *Eur. J. Biochem.* **1993**, *215*, 747−752.
(39) Witt, S.; Wohlfahrt, G.; Schomburg, G.; Hecht, H. J.; Kalisz, H. M. *Biochem. J.* **2000**, *347*, 553−559.
(40) Jin, L.; Yang, K.; Yao, K.; Zhang, S.; Tao, H.; Lee, S.-T.; Liu, Z.; Peng, R. *ACS Nano* **2012**, *6*, 4864−4875.
(41) Jones, M. N.; Manley, P.; Wilkinson, A. *Biochem. J.* **1982**, *203*, 285−291.
(42) Bovaird, J. H.; Ngo, T. T.; Lenhoff, H. M. *Clin. Chem.* **1982**, *28*, 2423−2426.
(43) Laurenti, E.; Suriano, G.; Ghibaudi, E. M.; Ferrari, R. P. *J. Inorg. Biochem.* **2000**, *81*, 259−266.
(44) Wang, C.; Tam, K. C. *J. Phys. Chem. B* **2005**, *109*, 5156−5161.
(45) Liang, Y.; Wu, D.; Feng, X.; Müllen, K. *Adv. Mater.* **2009**, *21*, 1679−1683.
(46) Mudhivarthi, V. K.; Cole, K. S.; Novak, M. J.; Kipphut, W.; Deshapriya, I. K.; Zhou, Y.; Kasi, R. M.; Kumar, C. V. *J. Mater. Chem.* **2012**, *22*, 20423−20433.
(47) Moehlenbrock, M. J.; Toby, T. K.; Waheed, A.; Minteer, S. D. *J. Am. Chem. Soc.* **2010**, *132*, 6288−6289.
(48) Agapakis, C. M.; Ducat, D. C.; Boyle, P. M.; Wintermute, E. H.; Way, J. C.; Silver, P. A. *J. Biol. Eng.* **2010**, *4*, 3−18.
(49) Wilner, O. I.; Weizmann, Y.; Gill, R.; Lioubashevski, O.; Freeman, R.; Willner, I. *Nat. Nanotechnol.* **2009**, *4*, 249−254.
(50) Fierobe, H. P.; Mingardon, F.; Mechaly, A.; Belaich, A.; Rincon, M. T.; Pages, S.; Lamed, R.; Tardif, C.; Belaich, J. P.; Bayer, E. A. *J. Biol. Chem.* **2005**, *280*, 16325−16334.
(51) Hyde, C. C.; Ahmed, S. A.; Padlan, E. A.; Miles, E. W.; Davies, D. R. *J. Biol. Chem.* **1988**, *263*, 17857−17871.

DOI: 10.1021/acscatal.5b00958
ACS Catal. 2015, 5, 4979−4988